A method to separate and quantify the effects of indentation size, residual stress and plastic damage when mapping properties using instrumented indentation

Hou, X & Jennett, NM

Original citation & hyperlink:
Hou, X & Jennett, NM 2017, 'A method to separate and quantify the effects of indentation size, residual stress and plastic damage when mapping properties using instrumented indentation' *Journal of Physics D: Applied Physics*, vol 50, no. 45, 455304
https://dx.doi.org/10.1088/1361-6463/aa8a22

DOI 10.1088/1361-6463/aa8a22
ISSN 0022-3727
ESSN 1361-6463

Publisher: IOP Publishing

A method to separate and quantify the effects of indentation size, residual stress and plastic damage when mapping properties using instrumented indentation

X D Hou[1,2] and N M Jennett[1]
1 Coventry University, Coventry, West Midlands, CV1 5FB, UK
2 National Physical Laboratory, Teddington, Middlesex, TW110LW, UK

Abstract

Instrumented indentation is a convenient and increasingly rapid method of high resolution mapping of surface properties. There is, however, significant untapped potential for the quantification of these properties, which is only possible by solving a number of serious issues that affect the absolute values for mechanical properties obtained from small indentations. The three most pressing currently are the quantification of: the Indentation Size Effect (ISE); Residual stress; and pile-up and sink-in – which is itself affected by residual stress and ISE. Hardness based indentation mapping is unable to distinguish these effects.

We describe a procedure that uses Elastic modulus as an internal reference and combines the information available from an indentation modulus map, a hardness map, and a determination of the ISE coefficient (using self-similar geometry indentation) to correct for the effects of stress, pile up and the indentation size effect, to leave a quantified map of plastic damage and grain refinement hardening in a surface. This procedure is used to map the residual stress in a cross-section of the machined surface of a previously stress free metal. The effect of surface grinding is compared to milling and is shown to cause different amounts of work hardening, increase in residual stress, and surface grain size reduction. The potential use of this procedure for mapping coatings in cross-section is discussed.

Key words: residual stress, indentation mapping, size effect, plastic damage

1. Introduction

Residual stress often exists in manufactured structures and components, playing an important role in their performance and lifetime. Depending upon the application, residual stress can be either harmful or beneficial to performance and service life. For example, compressive stress states impede crack formation and favourably displace the failure stress of a component. Various surface treatments are designed to manipulate stress states, examples include Nitriding (causing stress by material volume change), or the introduction of mechanical damage by shot or shock peening, etc. Alternatively steps, such as annealing, can be taken to reduce or even eliminate the residual stress that develops during manufacture. Residual stress may also be generated or altered whilst a component is in service. The measurement of residual stress is therefore important both for quality control and for structural monitoring. Accumulated plastic damage also leads to structural/component failure and structural monitoring to determine its work hardened state is critical to prediction of end of life. A method that is able to monitor both in a non-destructive way is highly sought after. The ISO technical report ISO/TR29381 [1] identified that instrumented indentation testing has the potential to do this via obtaining stress-strain curves but that procedures are needed to separate work hardening from the effects of stress on the indentation response.

Various quantitative methods exist to measure residual stress in both surfaces and bulk components, such as hole-drilling, X-ray, neutron diffraction etc. Laboratory X-ray sources are energy and intensity limited to penetration depths of microns; and measurements take a considerable time to perform. Brighter and higher energy X-ray sources are available at synchrotrons, but such scarce and expensive resources are not available for routine measurements. This is similarly the case for Neutron sources. Hole drilling is, therefore, the cheapest and easiest quantitative method to use, but suffers from being destructive and relatively low resolution. In contrast, instrumented nano-indentation testing (IIT) has high resolution, is also sensitive to residual stress, and is considered to be a low-destructive technique due to its small indent size. Various calibration methods have been published, aiming to produce a semi-quantitative map of stress, usually using hardness mapping [2,3,4,5] IIT is particularly useful when the stress state is driven by a large volume of material, as, although an elasto-plastic indentation causes a change to the stress and damage state very locally, it does not do enough damage to alter significantly the macroscopic average stress fields that are driving the residual stress. Most early work on the effect of residual stress on IIT focussed on hardness. Indeed, a casual expectation might be that yield stress should be offset by residual stress and that this is what is driving the hardness differences. Suresh and Giannakopoulos (1998) showed that, a comparison of stress-affected hardness measurements with an indentation made in a nominally zero stress region of a sample, allows a simple residual stress map to be generated relatively quickly and easily [6]. Hardness is, however, affected by many things, such as grain size, indentation size and dislocation density (work hardened state). This makes the use of hardness-derived residual stress maps unreliable.

A particular complication for hardness mapping is the well-known indentation size effect (ISE). We have previously reported that mechanical test results at small length-scales, both uniaxial [5] and hardness values obtained from instrumented nano-indentation [7, 8], are strongly dependant on a combined interaction of length scales such as grain size, indentation contact size and dislocation spacing. However, elastic modulus does not exhibit a size effect, except in the extreme case of nano-crystalline materials [9], where it has been shown that the increase in the volume fraction of grain boundary material does reduce the elastic modulus. In our previous ISE investigations it has become routine to use elastic modulus as an internal reference to insure against metrological errors (such as indenter area-function errors) and so to demonstrate that the measured ISE is real [10]. Typical hardness mapping is performed at constant applied force. This, however, causes hardness variation due to ISE. It is therefore essential to either quantify or control the ISE effect if hardness is to be used to map residual stress. The indentation size effect can be rapidly assessed using self-similar indentations in one spot, but it is the subject of ongoing research to use this information to specifically correct for ISE particularly, when there are other length-scales in the material that would interact with the ISE in a non-linear way and could be varying with position [11]. The simplest approach to this problem is to create maps using constant depth indentations, rather than constant maximum applied force. This provides a first order elimination of ISE variation, but it is not fool-proof if the sample is compositionally inhomogeneous and/or there is a large variation in pile up expected. Tsui et al. indented across the neutral stress axis in cross sections of bent beams and showed that both hardness and modulus results were affected by stress [2]. They found that, if the actual indentation contact area was measured and used in the data analysis, it generated both the stress-free modulus and the stress-free hardness of the material. Thus, it is not the stress itself that is being measured, but an error in the indentation contact area. This also explains why the observed changes in hardness and modulus due to stress are typically much larger than the size of the residual stresses involved.

The premise of this paper is that the parameter being affected by residual stress is the indentation contact area; compressive stress is equivalent to an increase in pile-up of the indentation and tensile stress equivalent to sink-in. Pile-up (or compressive stress) increases the measured stiffness of the indent but generates a reduction in the calculated indentation depth (hence the calculated contact area). The result of this is an increase in the measured modulus and hardness values. Tensile residual stress has an opposite effect on the modulus and hardness measurements (equivalent to sink-in). Thus, in a compositionally homogeneous sample, a ratio of elastic modulus values to the stress-free modulus value for the material gives a map of residual stress of the sample.

This paper shows that, by using the elastic modulus (rather than hardness) of a material as an internal calibration, it is possible to map residual stress and correct the hardness values to enable generation of a separate map of the plastic property changes of the material, which are also length-scale dependent.

2 Data Analysis Methodology

In order to separate out the influences of stress, indentation size effect, grain size refinement and plastic damage, the following data analysis methodology was developed:

1. Use ISO14577 standard methodology [12] to obtain the values of hardness and elastic modulus from indentations into a region of the sample that is nominally stress free. These indentations have to be over a range of indentation sizes in order to determine the stress free indentation size effect response of the material. The range of indentation sizes shall include any indentations sizes to be used later to map surface properties of the sample.
2. Check to ensure that the elastic modulus values obtained in step 1 are constant over the range of indentation sizes. If elastic modulus is not constant then this indicates possible compositional changes in the sample (requiring step 9), or an error in the instrument calibrations or indenter area function.
3. If the modulus values from step 1 are constant then the internal reference value, E_{ref}, for the sample is the arithmetic mean of the modulus values obtained in step 1. Note that this value includes and normalises the effect of any usual pile-up or sink-in exhibited by this sample.
4. Select a suitable indentation size to map the properties of the sample in the region of interest. Note that indentation separation resolution in the map shall be at least three indentation diameters. Other requirements of ISO14577 should also be taken into account, such as the size of indentations with respect to the sample surface roughness. The ISE hardness reference value H_{ref} is the hardness value obtained in step 1 at the indentation size selected. Where there is a lot of data scatter, H_{ref} may be obtained from a fit to the hardness vs. indentation depth data.
5. Obtain the indentation map using indentations of a set and constant depth, and calculate the values of hardness and elastic modulus according to ISO14577.
6. Take the ratio of the measured elastic modulus to the internal reference value obtained in step 3. Values less than unity indicate tensile residual stress; values greater than unity indicate compressive residual stress. A map of the ratio values is therefore a semi-quantitative map of the residual stress of the region of interest. In principle, comparison of results to known levels of residual stress can enable a calibration of the response to yield a fully quantified map of residual stress.

7. For each indentation, calculate the corrected indentation contact area, A_{cor}, using the equation (a rearranged form of ISO14577:2015 equation A14):

$$A_{Cor} = \pi \left(\frac{S}{2E_{ref}} \right)^2 \quad (1)$$

where S is the measured stiffness of the indentation.

8. Calculate the corrected hardness, H_{cor}, using the value of A_{cor} obtained in step 7.

$$H_{Cor} = \left(\frac{F_{max}}{A_{cor}} \right) \quad (2)$$

These values represent the plastic flow stress of the material at the indentation size selected for the map. A map of the ratio H_{cor} / H_{ref} shows where there are changes in the plasticity length scale of the region of interest. This can be attributed to either a change in dislocation density (e.g. due to work hardening) or a change in grain size, e.g. due to plastic damage [7].

9. In the case that there are known variations in the composition of the sample that are expected to cause a variation in elastic modulus, the simple calculation of E_{ref} and H_{ref} in step 3 and step 4 respectively is not valid. However, if the indentation contact sizes are measured directly (e.g. by Atomic Force Microscopy) then these values can be used to derive stress-corrected E_{ref} values and H_{ref} values that may then be used in the above procedure.

In this paper, the analysis was performed using ISO14577:2002 [13] and therefore plane strain modulus values were used throughout. It is noted that ISO14577:2015 uses a much improved contact mechanics analysis that uses an estimate of Poisson's ratio and the measured hardness and modulus ratio to correct for the change in contact area due to the lateral dilation of a material when indented. The procedure above is compatible with the use of either standard and the use of plane strain modulus or indentation modulus. The indentation size effect is not a measurement error but a genuinely harder response of the material and so ISE does not cause any problems when ISO14577:2015 uses the hardness to modulus ratio to correct for lateral dilation.

3 Experimental details

3.1 Specimen preparation and characterization

In this study, two 304 stainless steel specimens were taken from a batch that was originally selected to investigate the effect of surface preparation method on the susceptibility to stress corrosion cracking under simulated atmospheric corrosion conditions. The specimen preparation and characterization details are described elsewhere [14] but are summarized here. Prior to final specimen manufacture, the material was solution annealed to remove any residual cold work (at 1050°C for 30 minutes, followed by gas quenching). The first specimen was 'longitudinally ground' (LG) using standard machine shop procedures, such that grinding marks extended along the length of the specimen (see Figure 1). The second specimen was 'transversely milled' (TM) in a manner to simulate poor machine shop practice, such that milling marks are across the width of specimen. The specimens were then cross-sectioned, mounted in Bakelite resin and polished to study the underlying, near-surface material.

The microstructure was characterized by a Zeiss 'Supra 40' Field Emission Gun Scanning Electron Microscope (SEM) equipped with an electron back-scatter diffraction (EBSD) detector (Oxford Instruments Ltd, UK). The residual stress was determined using incremental hole-drilling measurements, according to the procedures outlined in NPL Good Practice Guide No 53 [15]. The

multi-axis strain gauges were installed with element 1 aligned along the sample length (longitudinal direction) and element 3 in the transverse direction, and the corresponding stresses presented as σ_1 and σ_3 as shown in Figure 1.

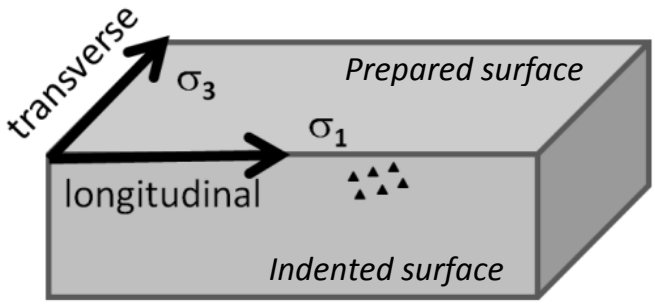

Figure 1 Sample schematic defining the grinding and stress directions with respect to the cross-section taken and indented. The hole-drilling hole was made in the top surface and yielded the orthogonal stress components σ_1 and σ_3. The indentations were therefore primarily affected by σ_1.

3.2 Nano-indentation

A Nanoindenter II (Nanoinstruments, USA) was used to perform indentation experiments on the samples in this study. Indentation was performed in a temperature-controlled laboratory (22.4 ± 0.1°C), using a Berkovich indenter (NPL unique reference code JEV) with a certified area function obtained by atomic force microscopy (AFM). Indents were placed in a square array, with a sufficient spacing that each indent did not interact with its neighbours. Indentations were performed in three regions as shown in Figure 2:

1. Initial indentations were performed under load control within the coarse-sized grains in the "far-field", i.e. sufficiently far away from the prepared surface to be in nominally unstressed, virgin material. A wide range of indentation sizes were obtained by using indentation maximum forces from 1 mN up to 100 mN. This provided an immediate estimate of the indentation size effect (ISE) and a base line of mechanical properties for material not affected by the surface machining.

2. High resolution indentation mappings were carried out within the "surface-damaged-layer" region. The recommended spacing of indentations in hardness standards such as ISO14577, is at least three indent diameters. High resolution is, therefore, not possible if the indents are in a line perpendicular to the interface. We adopted the strategy of rotating the indentation array to be at a 10° grazing incidence to the interface (see Figure 2) and by reducing the indentation size and spacing to the minimum. By selecting an area where the interface is relatively straight, it is then possible to order results according to perpendicular distance from the interface, which, therefore, enables much finer 'depth below surface' increments than would otherwise be possible. These indentations (within the surface damaged layer) were performed under load control, but with the indentation endpoint defined as a maximum indentation depth (100 nm or 150 nm depending on the size of the indentation and deformed layer thickness). In this way, the contribution of the ISE was kept constant by maintaining a constant contact size.

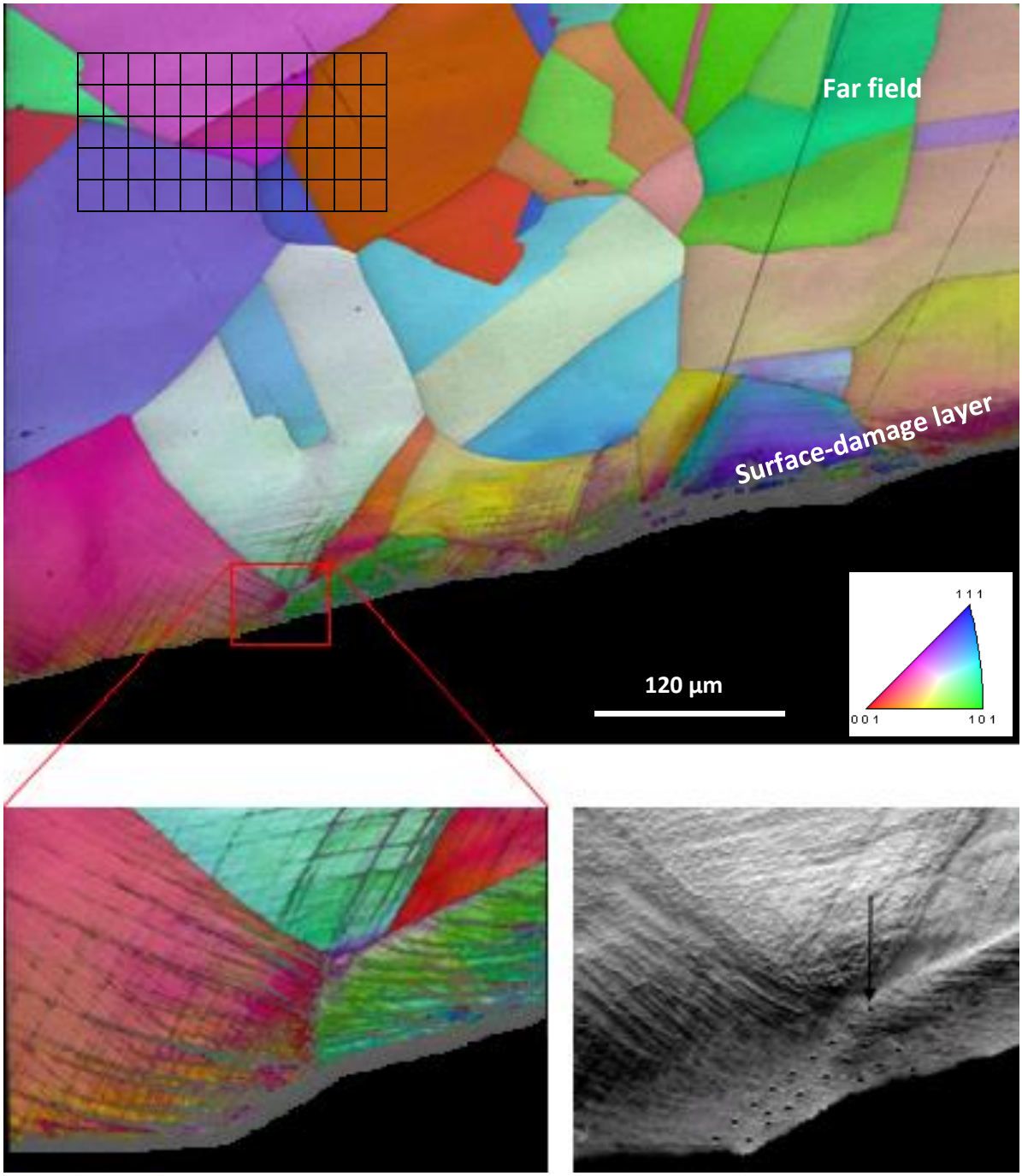

Figure 2 EBSD and SEM images of the TM specimen showing the indentation mapping near the surface (inverse pole figure colour scheme inserted). Two regions are defined. “Far-field”: a region is sufficiently far from the specimen surface to be undamaged by machining. The EBSD estimated grain size is approximately 250 µm. “Surface-damage layer”: the layer within the 20 µm region from the cross-section edge. Severe deformation was introduced into this layer including residual stress, grain refinement and possibly very high dislocation density. The imposed indentation grids (not scaled) are to illustrate the mapping used in the far-field and within the surface damaged layer. Indentations were sufficiently separated to avoid interference.

4. Results and discussions

4.1 EBSD mapping and residual stress measurements near-surface

EBSD maps of the TM specimen show an intensely deformed layer, of the order of 50 μm thick, near the prepared surface (see Figure 3). In this region, the milling process has broken the coarse grains into nano-crystalline grain structures with shear bands extending further into the material. The severe damage to the near-surface crystal structure makes it difficult for EBSD software to perform grain indexing. This is even more evident in the deformed layer of the LG specimen, which is approximately only 2 μm thick; no EBSD patterns could be generated from this layer at all.

The hole-drilling residual stress measurements are summarized in Figure 4. A hole was drilled into the machined surface of the sample and the strains resulting from the stress relief were measured using multi-axis strain gauges. Here, the stresses σ_1 and σ_3 represent the longitudinal and transverse stresses respectively (see Figure 1). Both specimens showed a high and similar transverse residual stress (σ_3) toward the surface. For the TM specimen, a transverse stress field is only observed within the first 50 μm region under the surface; while for the LG specimen, the stressed region extends 250 μm below the surface. Of more interest is the longitudinal stress, σ_1, as it is this stress component that affects the IIT results. In the LG specimen the longitudinal and transverse residual stress components are very similar; both showing a tensile profile. However, the longitudinal stress in the TM sample is very different. An extrapolation of the two measured points nearest the surface, back to the nominal surface position, suggests that there is a very small depth of tensile stress followed by a rapid transition to a compressive stress field extending about 300 μm below the surface. From the EBSD mapping, it is shown that the deformed layer of the milled specimen (TM) is much thicker than that of the ground specimen (LG).

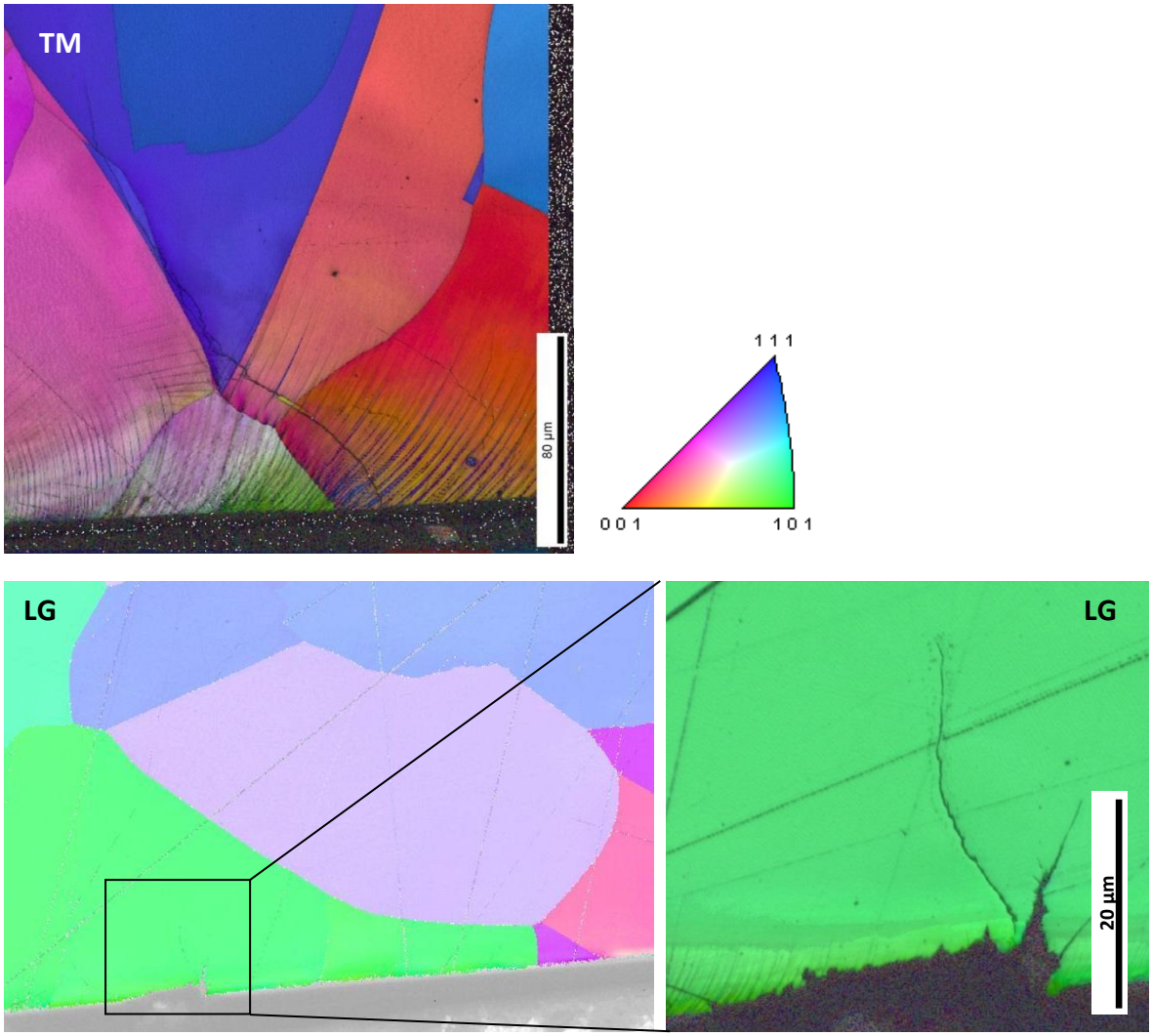

Figure 3 Electron back-scattered diffraction (EBSD) image of the TM specimen (top) and the LG specimen (bottom): showing highly deformed surface layers and shear bands (inverse pole figure colour scheme inserted).

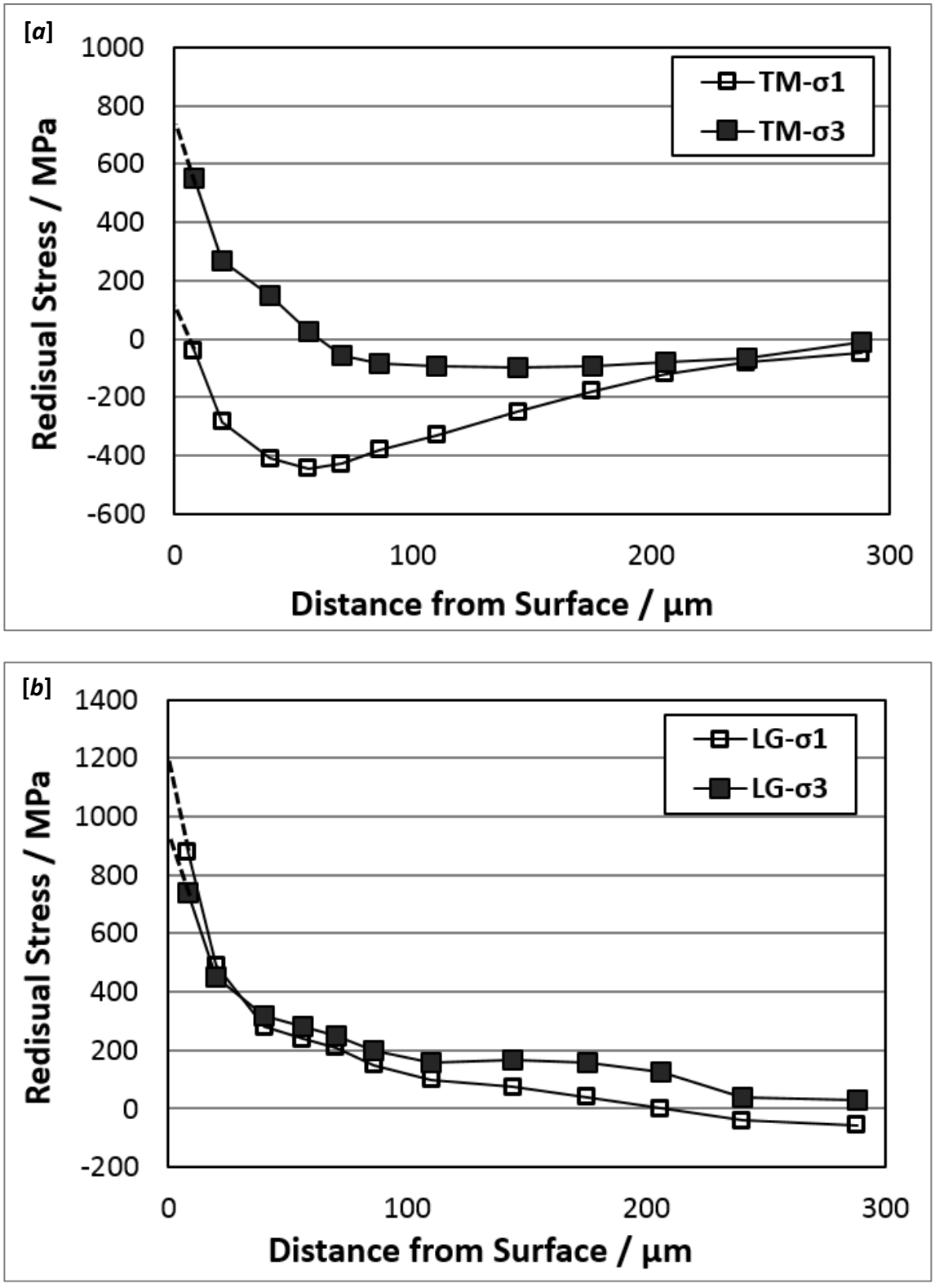

Figure 4 Hole drilling residual stress profiles for the milled specimen (TM) and ground specimen (LG) as a function of depth (redrawn from the literature reference [14]): the extrapolation (dotted line) to zero depth (surface position) indicates the stress at the surface that is measured by the indentation array. The stresses σ1 and σ3 represent the longitudinal and transverse stresses respectively, positive values indicate tensile stress and negative values indicate compressive stress state.

4.2 Indentation mapping within coarse grains

The indentation results from coarse grains, far away from the surface in both specimens, are summarized in Figure 5. The EBSD results showed that the grain size was large in these areas, typically 250 µm, with some grains as large as 1 mm (see Figure 2). The plane strain modulus is the same for all indentations in both samples. Obtaining a constant indentation modulus value with depth (in a homogeneous material) is a good indicator of valid measurements at all depths. The average of all the modulus values was calculated as a base line value (reference value) for the modulus of the unaffected material and was 202 GPa +/- 13 GPa. There is however, a significant increase in hardness as the indentation depth decreases from 1400 nm to about 30 nm. Since the grain size, at ~250 µm, is much larger than the indentation size (at least x25 greater), the increase in hardness is almost pure indentation size effect.

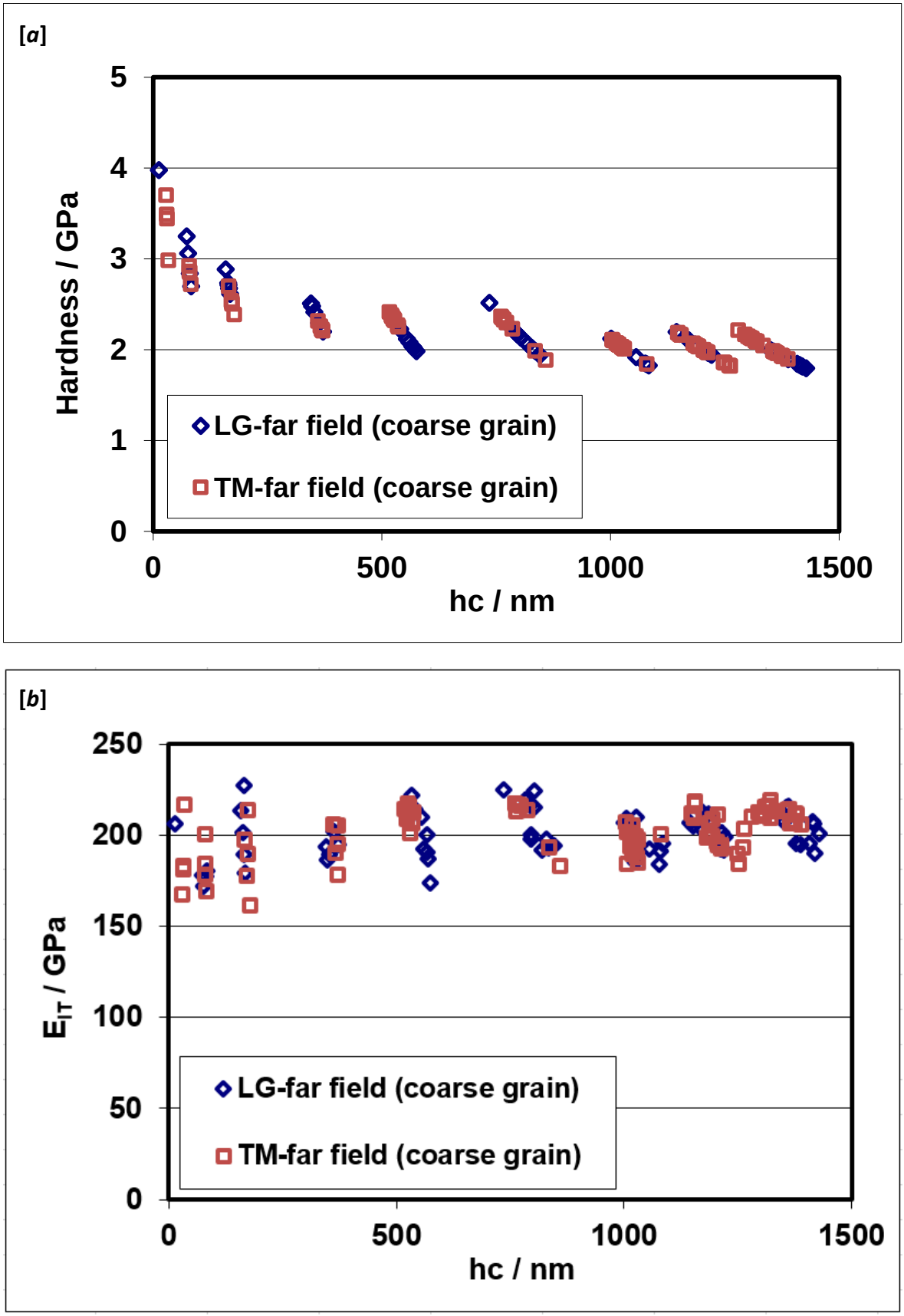

Figure 5 Hardness and plane strain modulus measured by instrumented indentation with load control to demonstrate the indentation size effect (ISE) of the "far-field region". Indentations of different sizes (forces from 0.1 mN to 100 mN) were used to study the indentation size effect. This is a typical output of step 1 of the method described in section 2.

4.3 Indentation mapping of the surface-damaged-layer region

SEM and EBSD of the indentation map near the surface of the TM specimen is shown in Figure 2 and confirms that the indentations were indeed within the deformed layer. These indentations were performed to a constant indentation depth of 150 nm; a lateral contact size of about 1 μm. Apart from any variation in pile-up, a constant indentation depth ensures that all the indentations made are the same size. This is necessary to maintain a constant contribution of the indentation size effect to the measured hardness value. This allows an assumption that any hardness difference observed across the deformed layer and into the bulk of the material can be attributed to residual stress and/or other size effects such as grain size or dislocation spacing.

Since the elastic modulus of a material is not significantly affected by residual stress, and the samples being investigated are homogeneous, the contribution of residual stress to the indentation measurements can be singled out by observing the plane strain modulus results. Figure 6 shows a drop in plane strain modulus within 10 μm of the surface of the TM sample. This is consistent with a tensile surface residual stress. Surprisingly, the hardness was found to be constant across the mapping region (see Figure 6). In this case, although a tensile residual stress should cause a low hardness measurement by instrumented indentation, the specimen preparation also produced a fine microstructure and work-hardening at the surface; these size effects are most likely compensating for the expected drop in hardness.

The same mapping procedure was conducted on the LG specimen, with the maximum indentation depth set to be 150 nm. The results are shown in Figure 7. Again, a significant reduction in plain strain modulus (from around 188 GPa to around 110 GPa) was measured close to the surface; however, the resolution was insufficient, as there were only a few measurement points in the region where the residual stress was significant enough to cause a decrease in modulus. This was addressed by reducing the maximum indentation depth from 150 nm to 100 nm, enabling a smaller spacing between indentations (4 μm). It was confirmed that the measured plane strain modulus was almost halved in the shallow layer, < 10 μm from the surface. This indicates a significant tensile stress in the LG specimen due to the surface preparation.

Direct comparison between the residual stress mapping from the hole-drilling technique and instrumented indentation technique is not readily possible, mainly due to the resolution difference. However, both of these techniques show a similar trend of progressively (towards the surface) increasing tensile residual stress in the near-surface, deformed layer. Hole drilling shows that the tensile residual stress (σ_1) in the LG sample (1200 MPa) is much larger than that in the TM sample (100MPa) and that there is a change in sign of the residual stress (σ_1) from tensile to compressive at about 10 μm below the TM surface. Indentation shows exactly the same trends: The drop in indentation plain strain modulus in the LG specimen is almost twice that measured in the TM specimen. The change from tensile to compressive stress in the TM sample can also be seen in the indentation plane strain modulus at approximately 10 μm from the surface, where the measured modulus value goes from below the reference modulus of 202 GPa to above (rises to ~211 GPa)

It can be seen that the indentation of the TM specimen shows a greater sensitivity to tensile stress than to compressive stress. The change in indentation plane strain modulus is greater in the first

10 µm depth below the surface than in the region 10 µm to 20 µm below the surface, whereas the hole-drilling measurement shows a bigger drop in σ_1 of the TM specimen between 10 µm to 20 µm. This difference in sensitivity is in agreement with results reported by Tsui et al. that the influence of stress is greater for specimens loaded in tension than those loaded in compression [2].

The plain strain modulus of the LG specimen increased as a function of depth below the surface but it only reached around 188 GPa within the measurement region. This is lower than the reference modulus of 202 GPa and is consistent with the hole drilling data, which shows continued tensile residual stress (σ_1) all the way to 250 µm below the surface.

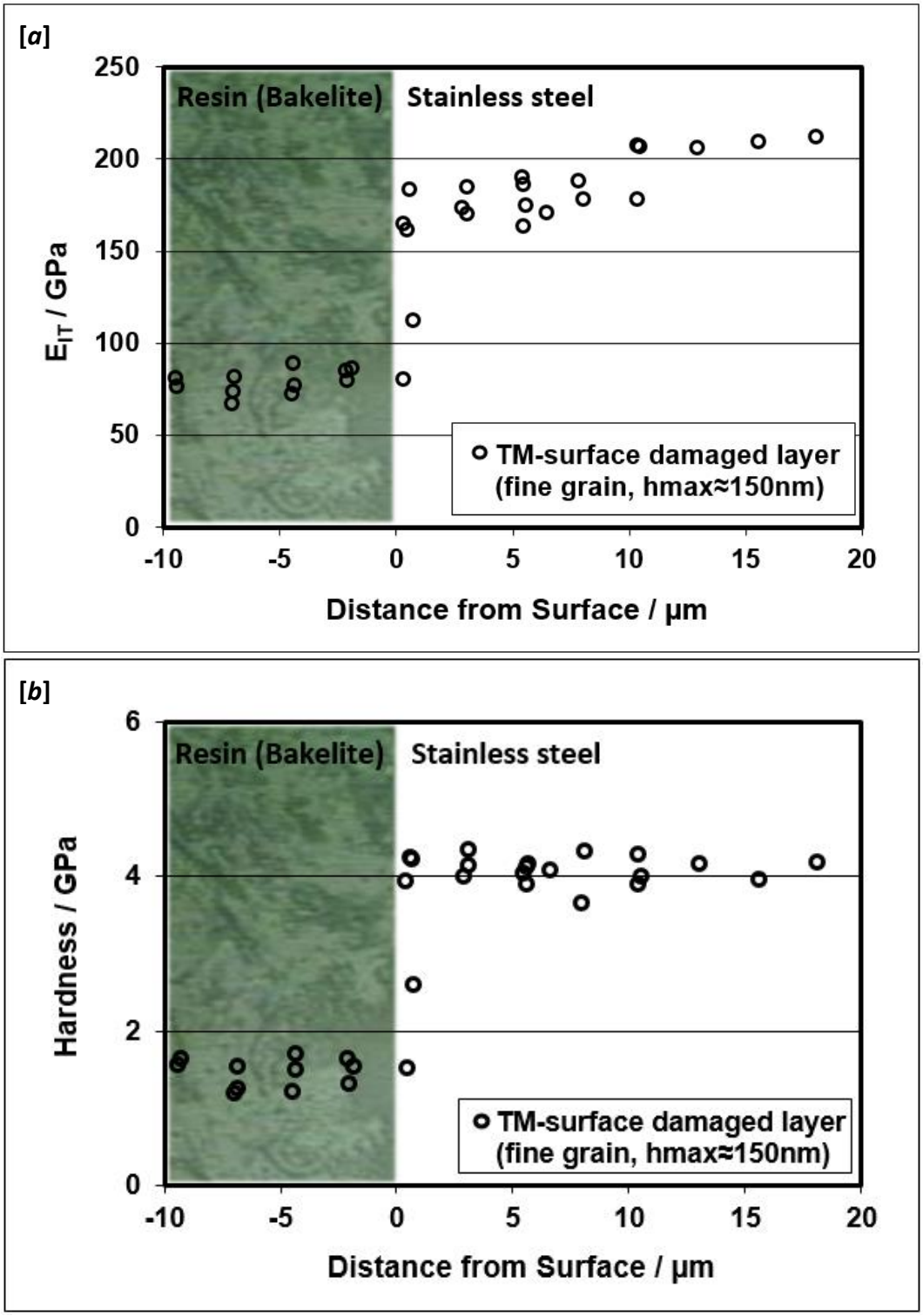

Figure 6 Size-controlled indentation of the damaged surface layer of the transversely milled (TM) specimen cross sections: Inclined rectangular arrays giving maps of indentation plane-strain modulus and hardness have been ordered by distance from the surface and projected onto a single axis to give indentation hardness and modulus at incremental distances (smaller than the indent separation) along a line perpendicular to the deformed surface layer. The maximum indentation depth was controlled to be 150 nm for all indents.

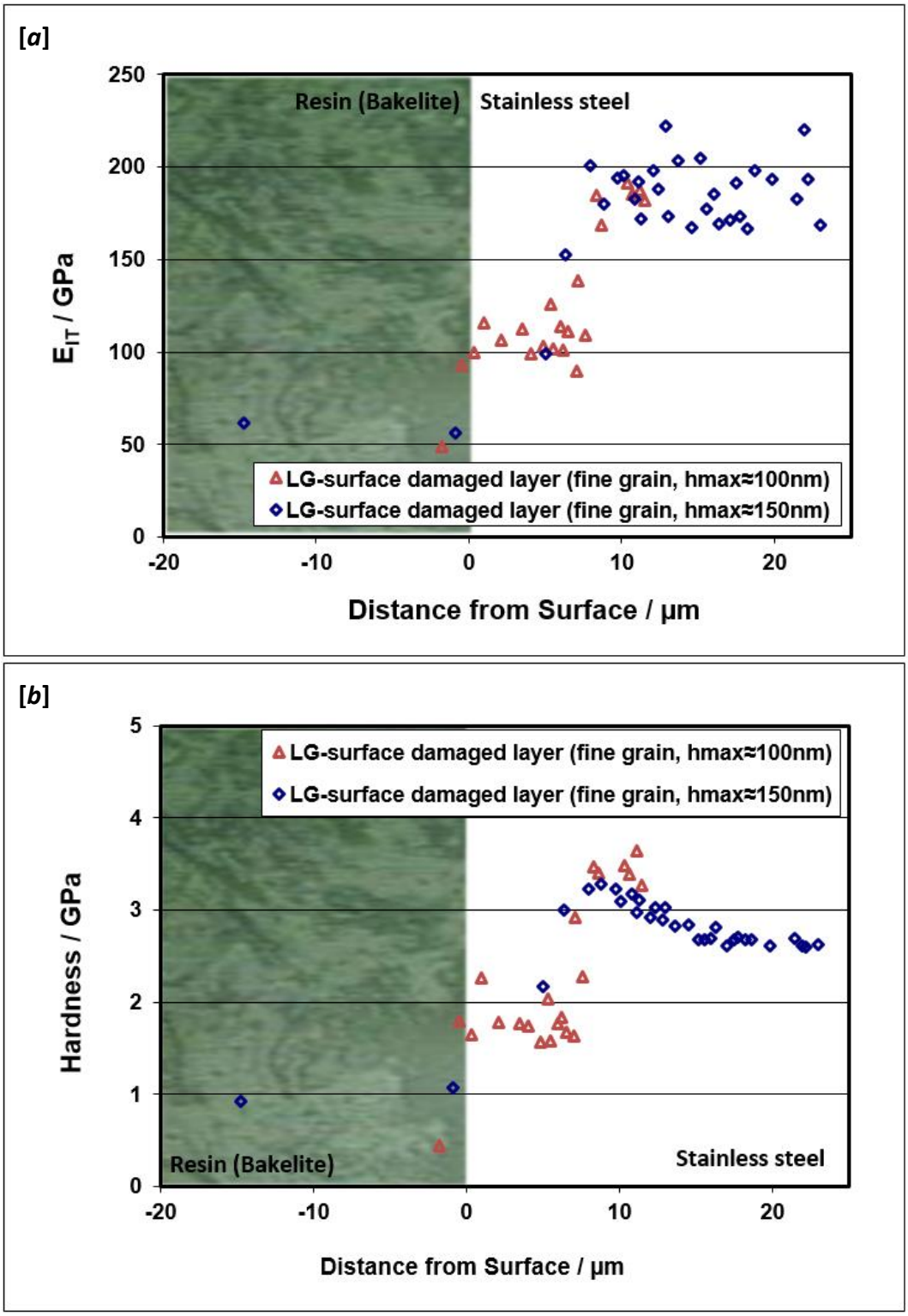

Figure 7 Size-controlled indentation of the damaged surface layer of the transversely ground (LG) specimen cross sections: Inclined rectangular arrays giving maps of indentation plane-strain modulus and hardness have been ordered by distance from the surface and projected onto a single axis to give indentation hardness and modulus at incremental distances (smaller than the indent separation) along a line perpendicular to the deformed surface layer. The max indentation depth was controlled to be 150 nm initially, with additional smaller indentations (100 nm deep) added to increase the near-surface resolution.

4.4 Indentation mapping of residual stress corrected plasticity information

It has been indicated earlier that the use of simple hardness maps is unreliable and can be misleading. The potential for confusion is clearly demonstrated in the results obtained here. If hardness values are used without correction, a strange trend is observed in the as-measured hardness as a function of depth below the surface of the LG sample, see Figure 7b. The surface hardness is depressed and increases to a maximum at 10 µm below the surface, before decreasing again. If hardness were the only issue, then this might be misinterpreted as a layer of harder material below the surface of the sample, or a stress distribution with a maximum stress below the sample surface. This is not the case and the apparent maximum is the interplay between two effects: a hardness (reduced by stress at the surface) rising with depth below the surface; and a hardness increase at the surface (due to grain size reduction and/or dislocation density at the surface due to the machining) decaying with depth into the material. The hardness data corrected for the effects of residual stress (and pile up) is shown in Figure 8. Data sets for 150nm deep indents into both samples are shown along with the 100nm deep indentations made into the TM sample. The H_{ref} values obtained for the 150 nm indentation sizes used are plotted in Figure 8 as a comparison. The average hardness for 1400 nm indents is also shown to indicate the relative contribution of ISE to the hardness values. The corrected hardness values clearly reveal that the maximum of plastic damage is at the surface as expected, and decays with depth into the surface for both samples (LG and TM). This further demonstrates the more subtle case of the apparently constant uncorrected hardness of the TM sample being misleading in Figure 6b. In this case, the effects of stress and plastic damage are exactly compensating to give an appearance of constant hardness.

From indentation data alone, it is not possible to know whether the higher corrected hardness of the surface is due to work hardening or to grain size refinement or both. The EBSD images, however, clearly show grain refinement to be occurring and that the combination of grain refinement and work hardening at the surface was so extreme that the grain orientations (and so grain size) became unmeasurable. It was, therefore, not possible to make an estimate of the relative contributions of grain size and work hardening and this will generally be the case where there is no means of grain size measurement in the region indented. It is interesting that the corrected hardness remains above the H_{ref} values throughout the range plotted in Figure 8 (up to 25um below the surface), indicating that plastic damage caused by the surface machining is present in both samples to at least these depths, which is consistent with the SEM and EBSD images in Figure 3.

In this paper we were able to assume that the material was compositionally (elastically) homogeneous and that we were able to identify and indent a stress free area to get a reference value for the material plane strain modulus. However, Tsui et al. have shown that direct measurements of the contact area can be used to correct indentation results to give a stress free plane strain modulus. Thus, if each indentation area of contact is directly measured (e.g. by AFM), the method in this paper does not have to be limited to homogeneous materials – mapping of inhomogeneous materials is also possible. In this case, the ratio of the directly measured contact area and the indentation contact mechanics calculated area gives a semi-quantitative measure of the stress component.

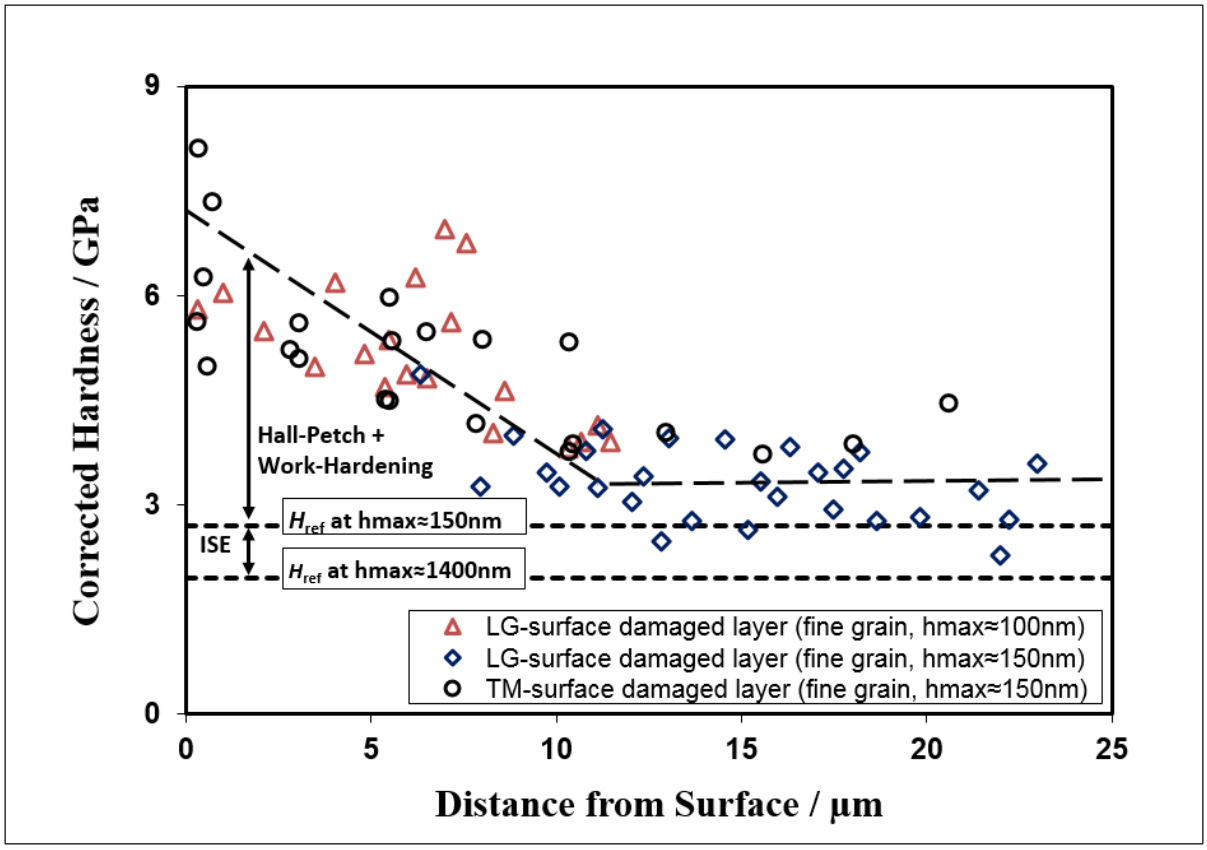

Figure 8 Cross-sectional depth-profile plots of hardness data corrected for the effect of residual stress by using far field modulus as an internal reference. Each depth profile was performed at a constant indentation depth and the contribution of indentation size effect to the measured hardness is shown. Depth profiles in both LG and TM samples show a maximum plastic damage (Hall-Petch plus work hardening) at the surface, which decreases with depth below the surface.

An important case of inhomogeneous material is the cross-section of a coating. This method could be applied to indentation maps of coatings cross-sections. Easiest to obtain is information about the stress field, hardness and modulus in the substrate, because it is likely that an indentation far from the coating interface could be stress free and could therefore supply the necessary internal stress free reference modulus (as in this paper). Separation of elastic modulus, stress and hardness from indentation maps of the coating material in cross-section requires either indentation information from unstressed coating material, an independent value for coating modulus, or direct measurement of indentation size to obtain a corrected modulus and therefore the stress and hardness measurement of the coating. The small thickness of a thin coating may make it difficult to obtain enough indentation size effect information to estimate the hardness of the coating material (unaffected by the indentation size effect). This method may also be used to map the stress, modulus and hardness in the plane of a nominally homogenous surface if the modulus is known or a portion of unstressed surface can be indented, or, alternatively, a direct measurement of indentation size can be obtained to provide a reference modulus (or directly correct the modulus and hardness measurements). Laterally inhomogeneous surfaces could also be measured but, where there is likely to be unknown inhomogeneity in the indentation depth direction, it would be impossible to know if a different property material immediately below the indent was causing a difference in modulus value or not.

The findings in this paper have important implications for the measurement of coatings' properties in plan. Strictly the indentation of coatings standard ISO14577-4 [16] cannot be used if there is residual stress, however, further work is called for to verify if this restriction may be lifted when the indent size is directly measured.

It should also be noted that, in general, ISO14577-4 does not take indentation size effects into account:

- Coating hardness is identified by determining the indentation depth at which the substrate makes a significant contribution to the hardness result.
- Coating-only modulus is obtained by deconvoluting it from the depth-dependent combination of two moduli – the substrate and the coating.

Indentation size does not affect the measurement of elastic modulus but does need to be addressed when quoting hardness values. Conversely, thinner coatings are genuinely harder, for the same reasons that smaller indentations are harder. The concept that hardness is fundamentally length-scale dependent presents a real problem when comparing hardness data from indents of different sizes and contradicts the idea that smaller indents always give better hardness information from a coating; the indentation response will be a result of the combined indent and coating sizes and very small indents will generate artificially high hardness values compared to those representative of the coating performance. The strategy demonstrated here (of comparing like-sized indents) is strongly recommended for comparison of all coating hardness results.

4. Conclusions

This is the first paper to our knowledge that provides a valid analysis to separate and quantify plasticity size effect (including grain refinement and hardening due to increase in dislocation density), indentation size effect (an issue particularly important for high resolution mechanical property mapping) and residual stress (often involved in machining and heat treatment) for mechanical property mapping. We have shown that uncorrected hardness maps are unreliable and misleading. They are unable to map combinations of residual stress and plastic damage. Unfortunately this combination is the most likely situation driving the need for surface property mapping.

We have developed and demonstrated a new procedure to quantify and correct for the effects of residual stress on indentation measurements. This uses the elastic modulus of a material as an internal reference. Elastic modulus is derived from bond strength and crystal coordination number and may safely be assumed to be unaffected by plastic damage, residual stress, and has no intrinsic indentation size effect associated. The method shows the benefits of making indentation maps at constant depth (rather than constant force). This new approach allows a direct estimate of the indentation size effect on the mapped hardness values and allows separation of ISE from other length-scale effects such as grain refinement.

We have presented a case study of the surface machining of 304 stainless steel and shown that this induces residual stress, grain refinement and work hardening into and below the surface. The indentation derived map of residual stress is entirely consistent with independent measurements of residual stress by hole-drilling. The comparison of uncorrected with corrected hardness maps demonstrates the requirement to use our new procedure, if valid conclusions regarding the stress and or damage state of a material are to be made. This new procedure, presented here, provides a rapid, high resolution, essentially low/non-destructive method to map the stress and plastic damage of a

surfaces (and coatings) in plan or in cross-section. The method is particularly useful in cross-section and where the material is homogenous in composition, but can be extended to inhomogeneous materials and coatings by the use of direct indentation size measurement.

Acknowledgement

This project has received funding from the EMPIR programme co-financed by the Participating States and from the European Union's Horizon 2020 research and innovation programme. The authors acknowledge the contributions of: Dr Alan Turnbull (provision of samples and hole-drilling data), Dr Ken Mingard (generation of the EBSD data) and Dr Jerry Lord for useful discussions.

References

[1] ISO/TR 29381:2008, Metallic materials -- Measurement of mechanical properties by an instrumented indentation test -- Indentation tensile properties
[2] T.Y. Tsui, W.C. Oliver and G.M. Pharr, *J. Mater. Res.* **11** (1996) p.752-759
[3] J. G. Swadener, B. Taljat and G.M. Pharr, *J. Mater. Res.* **16** (2001) p.2091-2102
[4] J. Dean, G. Aldrich-Smith and T.W. Clyne, *Acta. Mater.* **59** (2011) p.2749-2761
[5] J. Jang, *J. Ceram. Process. Res.* **10** (2009) p.391-400
[6] S. Suresh and A.E. Giannakopoulos *Acta Mater.* **46** (1998) p.5755-5767
[7] X.D. Hou and N. M. Jennett, *Acta Mater.* **60** (2012) p.4128-4135
[8] X.D. Hou, A.J. Bushby and N.M. Jennett, *J Phys D Appl Phys* **41** (2008) p.074006
[9] D.C. Hurley, R.H. Geiss, M. Kopycinska-Müller, J. Müller, D.T. Read, J.E. Wright, N.M. Jennett and A.S. Maxwell, *J. Mater. Res.* **20** (2005) p.1186-1193
[10] X.D. Hou, N.M. Jennett and M. Parlinska-Wojtan, *J. Phys. D Appl. Phys.* **46** (2013) p.265301
[11] http://empir.npl.co.uk/strength-able/
[12] ISO 14577-1&2:2015, Metallic materials – Instrumented indentation test for hardness and materials parameter
[13] ISO 14577-1&2:2002, Metallic materials – Instrumented indentation test for hardness and materials parameter
[14] A. Turnbull, K. Mingard, J.D. Lord, B. Roebuck, D.R. Tice, K.J. Mottershead, N.D. Fairweather and A.K. Bradbury, *Corros. Sci.* **53** (2001) p.3398–3415
[15] P.V. Grant, J.D. Lord, P. Whitehead , NPL Good Practice Guide No. 53 - Issue 2, 2006
[16] ISO 14577-4:2016, Metallic materials – Instrumented indentation test for hardness and materials parameter-Part4: Test method for metallic and non-metallic coatings